Spatial Spectrum Holes in TV Band: A Measurement in Beijing

Sai Huang(✉), Yajian Huang, Hao zhou, Zhiyong Feng, Yifan Zhang, and Ping Zhang

Key Laboratory of Universal Wireless Communications Ministry of Education, Wireless Technology Innovation Institute (WTI), Beijing University of Posts and Telecommunications, Beijing, China
huangsai@bupt.edu.cn

Abstract. Spatial spectrum holes are areas where TV signal strength falls below a certain threshold and TV frequency can be utilized without license. In our measurement, we prove the existence of spatial spectrum holes considering shadowing and building penetration. To evaluate the influence of shadowing, two dimensional radio environment mapping (REM) is constructed for a $500\,m \times 530\,m$ area in the downtown. According to the REM, a maximum attenuation of 30 dB can be caused by building blockage and shadowing. To measure the loss of wall penetration, a three dimensional measurement is conducted in the outer and inner area of a 12-floor building. It is found that the wall attenuation approximately follows a normal distribution with a mean of 24.31 dB. The distribution of spatial spectrum holes is then plotted indicating spatial spectrum holes are abundant especially in the outskirts of Beijing.

Keywords: TV white space · Spectrum measurement · Radio environment mapping · Spatial spectrum access opportunities

1 Introduction

TV band is considered most suitable for spectrum relocation and measurements were conducted all over the world to check the feasibility of CR (cognitive radio) in TVWS (TV white space). Islam *et al.* in [1] reported the utilization of TV band is only 52.35% in Singapore while Bao *et al.* in [2] found the utilization of TV band is 54.78% in Vietnam. In these measurements, spectrum holes are considered as the time and frequency on which TV tower is not transmitting. However apart from time and frequency domain spectrum holes, there are also spectrum holes in the spatial domain. According to FCC regulation, devices can utilize the TV band in areas where TV signal strength falls below −114 dBm even if TV tower is transmitting [3]. Since the aforementioned measurements are

This work was supported by the National Natural Science Foundation of China (61227801, 61421061), the National Key Technology R&D Program of China (2014ZX03001027-003).

M. Weichold et al. (Eds.): CROWNCOM 2015, LNICST 156, pp. 585–592, 2015.
DOI: 10.1007/978-3-319-24540-9_48

all conducted at fixed locations with good TV signal coverage, they are unable to reveal the geographical aspects of spectrum holes.

Chen *et al.* in [4] conducted a mobile measurement in Beijing and predicted the signal strength with large-scale propagation model. They found the TV signal strength is above −85 dBm all over Beijing. Although there are no large spatial spectrum holes according to Chen, there may be small outdoor spatial spectrum holes because of shadowing and indoor spatial spectrum holes caused by wall attenuation.

This paper studies the existence of spatial spectrum holes in Beijing by measuring the typical shadowing and wall attenuation condition in the city. To evaluate the influence of shadowing, radio environment mapping (REM) is constructed for a $500m \times 530m$ area in the downtown. To measure the loss of wall penetration, three dimensional measurement is conducted in the outer and inner area of a 12-floor building. The wall attenuation is then calculated and approximated as a normal distribution. Utilizing the calculated value of shadowing and wall attenuation, the geographical distribution of spatial spectrum holes is plotted on the basis of the large-scale fading result of Chen.

The rest of the paper is organized as follows. Section 2 introduces the measurement of shadowing. The measurement of wall attenuation is presented in Section 3. Section 4 demonstrates the geographical distribution of spectrum holes and Section 5 concludes the paper.

2 Measurement of Shadowing

Signal strength may attenuate a great deal due to shadowing caused by building blockage. To investigate the effect of shadowing in downtown Beijing, REM is constructed for a typical area of the city.

2.1 Measurement Setting

The measurement region is a university located on the 3^{rd} ring of Beijing and the coordinate is 116.348345E and 39.967108N. The shape of the area is almost rectangular with a length of 530 meters and width of 500 meters as illustrated in Fig. 1. The buildings in the area are mostly between 6-floor and 15-floor in height, which is typical of downtown Beijing. The university has two main landscapes, i.e., dense residential area in the north and open playground in the south (see Fig. 1).

In China, the $470 - 806$ MHz spectrum band is allocated for terrestrial TV broadcasting and the bandwidth of each TV channel is 8 MHz. As measurement needs to be taken at a large number of sampling points in REM, only channel 22 ($478-486$MHz) was measured. Channel 22 is utilized by digital TV broadcasting and is transmitting in the entire measurement period.

Measurement equipment includes Anritsu MS2720T handheld spectrum analyzer and omnidirectional broadband antenna BOGER DA753G. The antenna is connected to the spectrum analyzer by a low-loss cable and kept three meters

above the ground in the measurement. The resolution bandwidth (RBW) of the spectrum analyzer is set as 200 kHz. Signal strength is measured at each position 200 times and averaged to eliminate the fluctuations caused over time. Moreover, the Global Positioning System (GPS) module inside MS2720T is utilized to ensure that measurement is taken at the pre-selected positions.

2.2 Simulated Annealing Assisted Electron Repulsion

Generally, REM is conducted in two steps, i.e., sampling and interpolation. Signal strength is first measured at a number of sampling points and then interpolation is utilized to estimate signal strength of the entire area. The most commonly utilized sampling algorithm is symmetric sampling which places sampling points on a uniform grid. In our scenario, symmetric sampling usually put sample points in inaccessible areas, for example inside buildings, as illustrated by the yellow dots in Fig. 1. Therefore a novel sampling algorithm named simulated annealing assisted electron repulsion (SAER) is proposed.

In SAER, the sampling points and boundaries of inaccessible areas are treated as electrons such that the repulsive force between them can ensure the uniform distribution of sampling points and keep them out of inaccessible areas simultaneously. Initially, M fixed electrons are put uniformly on the boundaries of inaccessible areas and N free electrons are deployed in the sampling area at random positions. There are $M+N-1$ Coulombic forces on each electron. The resultant of Coulombic forces $\mathbf{F}_i$ on the i^{th} electron e_i (at position $\mathbf{r_i}$) is

$$\mathbf{F}_i(\mathbf{r}) = \xi \cdot Q_i \cdot \sum_{j=1, j\neq i}^{N+M} Q_j \frac{(\mathbf{r_i} - \mathbf{r_j})}{\|\mathbf{r_i} - \mathbf{r_j}\|^3}, \tag{1}$$

where ξ is the Coulombic constant, Q_i and Q_j are the quantities of e_i and e_j respectively. Assuming the Coulombic forces on each electron is constant in a short interval Δt, the displacement of the electron is

$$\mathbf{L_i} = \mathbf{v}_i \cdot \Delta t + \frac{1}{2} \cdot \mathbf{a}_i \cdot \Delta t^2, \tag{2}$$

where $\mathbf{a}_i$ is the acceleration caused by the Coulombic forces. Utilizing (2), the position of the i^{th} electron after Δt can be calculated. The displacement process can be carried out iteratively until the resultant forces approach zero, which suggests the sampling positions reach a relatively stable distribution.

In addition, simulated annealing is adopted to prevent the sampling position from converging to local optimal. The objective function is chosen as

$$\Phi(S) = \Delta F_i^{k+1} = \left\|\mathbf{F}_i^{k+1}\right\| - \left\|\mathbf{F}_i^{k}\right\|, \tag{3}$$

where $\mathbf{F}_i^k$ and $\mathbf{F}_i^{k+1}$ are the resultant of Coulombic forces on i^{th} electron in the k^{th} and $(k+1)^{th}$ iteration. The probability of accepting a new state is given by

$$P\left(S_i \rightarrow S_{i+1}\right) = \begin{cases} 1 & \Phi(S_{i+1}) \leq \Phi(S_i) \\ e^{\frac{\Phi(S_i)-\Phi(S_{i+1})}{T}} & \Phi(S_{i+1}) > \Phi(S_i), \end{cases} \tag{4}$$

where S_i and S_{i+1} denote the former and current positions of the electron respectively. T is the system temperature which goes to zero. In an iteration, if the new state is accepted, the electron is moved to position S_{i+1}. Otherwise, the position of the electron stays unchanged.

In Fig. 1, the sampling points generated using SAER is marked by red dots. It can be clearly recognized that all the positions are placed outside the inaccessible area and the distribution is approximately uniform.

Fig. 1. Sampling Points Distribution in REM

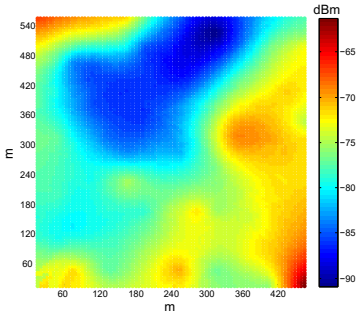

Fig. 2. REM of the Selected Area

2.3 Results Analysis

After measuring signal power at 64 sampling points, Kriging interpolation is used to estimate the signal strength of the entire region. To validate the accuracy of our REM, signal strength of 80 randomly chosen positions (verification points) are measured. Mean relatively error (MRE) is adopted to assess the accuracy and can be defined as follows.

$$MRE = \frac{1}{N}\sum_{n=1}^{N}\frac{|P_n^* - P_n|}{P_n}, \tag{5}$$

where $P_n{}^*$ is estimated signal strength at the the n^{th} verification point and P_n is the measured value. The MREs of SAER and symmetric sampling are 4.72% and 6.58% respectively. Since some sampling points generated by symmetric sampling are inaccessible, we replaced them with their nearest accessible points.

The resultant REM is plotted in Fig. 2. The maximum signal strength comes from the southeast corner of the university (−60 dBm), where a playground locates. The northern part has many tall buildings and experiences the minimum

signal power (approximately −95 dBm). It is shown that the signal strength fluctuates between −95 dBm and −60 dBm. If there is no shadowing, signal strength of the entire area would be approximately the maximum value (−60 dBm). Because of shadowing of different degrees, signal strength is distributed in a wide range. With strong shadowing, the variation of signal strength can be more than 30 dB even in a small area.

3 Measurement of Building Penetration Loss

Although signal strength estimated by large-scale measurement is much higher than the threshold defined by FCC, indoor spatial spectrum holes may appear owing to building penetration loss. To figure out the influence of building penetration loss, a three dimensional measurement is conducted for a typical building in Beijing.

3.1 Measurement Settings

The measurement is conducted in a 12-floor masonry building located in the university mentioned in the previous measurement. The building mostly consists of concrete, brick and coated windows, which is typical for northern China. The shape of the building is irregular as illustrated in Fig. 3.

Since a number of positions need to be measured, only channel 22 is measured. Measurement equipment and their connection are also similar to the previous section. Since GPS fails to work in the inner area of the building, the measurement positions are acquired with the help of a tachometer. The measurement equipment is kept in a chart to move around.

To limit the complexity of the measurement, we choose the 4^{th}, 7^{th}, 9^{th} and 12^{th} floor and the surface of building to conduct our measurement. The surface of building has the strongest signal strength since it is free from wall attenuation. The 4^{th}, 7^{th}, 9^{th} and 12^{th} floors are the inner area of the building.

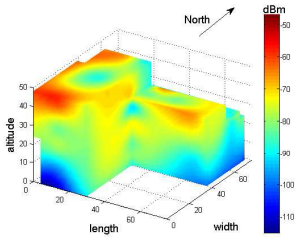

Fig. 3. Outdoor Signal Strength

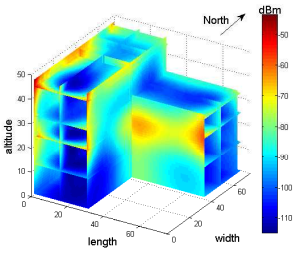

Fig. 4. Indoor Signal Strength

3.2 Results Analysis

With the recorded signal strength at the sampling points, Kriging interpolation is utilized to estimate signal strength in entire area. Another 180 randomly chosen locations is also measured to verify the accuracy of our estimation.

The estimated signal strength for the outer and inner area of the building are plotted in Fig. 3 and Fig. 4. The MREs for both the inner and outer area are all 5.9%, indicating our estimation is reliable.

Fig. 3 shows that the signal strength of the southwest part is higher than the northeast. This is because the southwest part is facing radiation and it further validates that shadowing aggravates the attenuation of signal strength. The signal strength on the roof (−60 dBm) is 45 dB higher than the bottom.

From the vertical view, signal strength is strongly related with the height or floor of the measurement positions. Generally speaking, signal strength increases with height. From the horizontal view, signal strength of innermost spots (−120 dBm) is 50 dBm lower than the outermost ones.

3.3 Analysis of the Penetration Loss

The existence of spatial spectrum holes is strongly related to the penetration loss. Therefore We analyze two kinds of penetration loss, i.e., wall penetration loss (WPL) and floor penetration loss (FPL) and denote them as l_{wpl} and l_{fpl}.

Wall Penetration Loss. Fig. 5 shows the statistical histogram of the WPL, which resembles a normal distribution. To assess the normality of the WPL, Kolmogorov-Smirnov(K-S) test is conducted at significance level ($\alpha = 0.02$), wherein the empirical PDF is compared to a normal PDF with the mean and standard deviation estimated from the measured data. As the fitting curve indicates, the WPL can be well approximated by a Gaussian distribution expressed by (6).

$$p(l_{wpl}) = \frac{1}{\sqrt{2\pi\sigma^2}} \exp(-\frac{(l_{wpl} - u)^2}{2\sigma^2}), \tag{6}$$

where $u = 24.31$ and $\sigma = 5.12$. This indicates that the average attenuation caused by WPL is approximately 24 dB, which is 1 dB higher than the value reported by FCC [3]. This difference can be explained by the difference in construction material in different countries.Therefore it is necessary to make adjustments when applying FCC regulations in China.

Floor Penetration Loss. Fig. 6 shows the FPL as a function of the number of ceilings between the measurement site and the roof. It can be seen that the FPL increases almost linearly with the number of floors. Hence a linear model for FPL is assumed as follows.

$$l_{fpl} = l_o + \kappa \cdot n_{FL} + \xi, \tag{7}$$

where l_o is the initial value and κ is the increase in loss per floor, n_{FL} is the number of ceilings signal passes through and ξ is the statistical variation.

Linear least-square regression is utilized to calculate l_o and κ. The resultant l_o and κ are 5.31 dB and 15.49 dB respectively. The goodness of fit measured by Root Mean Square Error (RMSE) is 0.4413. From our analysis, a 20.8 dB loss exists when signal penetrates the ceiling between two floors. Our result is 2.5 dB higher compared to COST231 [5], which can be explained by the fact that the interlayer may be thicker in Beijing.

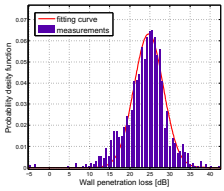

Fig. 5. Cumulative Distribution Function of WPL

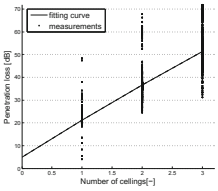

Fig. 6. Model of FPL for Different Number of Floors

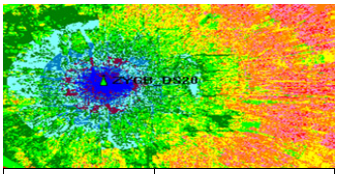

Signal strength (dBm)	Probability distribution of spatial holes
(-∞,-90)	100%
(-90,-85)	100%
(-85,-80)	100%
(-80,-75)	97%-100%
(-75,-70)	80%-97%
(-70,-65)	46%-80%
(-65,+∞)	0%-46%

Fig. 7. The probability distribution of spatial holes in Beijing

4 Distribution of Spatial Spectrum Holes

Chen *et al.* conducted a mobile measurement to check the geographical distribution of TV signal strength. However, their results consider only large scale fading. As shadowing and wall attenuation also contribute to loss in signal strength, spatial spectrum holes may appear. Since shadowing and wall attenuation loss are all random variables, the probability that spatial holes exist can be calculated as follows.

$$P_{holes} = \int_{p-\varepsilon-l_s}^{+\infty} \int_{0}^{+\infty} f(l_{wpl}, l_s) dl_{wpl} dl_s, \tag{8}$$

where $f(l_{wpl}, l_s)$ is the joint probability density function of the WPL and shadowing, while p is the signal strength predicted by large scale fading and ε is the threshold for spatial spectrum hole. According to FCC regulation, ε is -114

dBm. However, the minimum working power level for digital TV is −90 dBm according to Chinese standard [6]. Analog TV makes even looser requirement about working power level. The −114 dBm threshold required by FCC should be relaxed in China.

Since there is no official regulation about the threshold in China, a −95 dBm threshold is assumed. As shadowing is tightly coupled with the blockage condition and its distribution is relatively complex, a fixed shadowing loss of 5dB is adopted. In this case, the probability of spatial spectrum holes is determined by the distribution of wall attenuation.

The probability distribution of spatial spectrum holes is plotted in Fig. 7, with different colors denoting different probabilities of spatial holes. In the central area of the city, TV signal strength is strong and the probabilities of spatial spectrum hole is low (the blue areas). However, most areas of the city have at least 80% probability of spatial spectrum holes. In the outskirt, where the signal strength is below −75 dBm, spatial spectrum holes are very abundant.

The spatial spectrum holes are mostly caused by wall attenuation and appear in indoor areas. Therefore we call them indoor spatial spectrum holes, which can be used by the short-range communication such as Wi-Fi or dense small cell deployment in 5G.

5 Conclusion

In this paper, we conducted a comprehensive measurement in TV band in Beijing to validate the existence of spectrum holes in the spatial domain. With radio environment mapping, we show that a variation of 30 dB in signal strength can be caused by building blockage and shadowing. By measuring the inner and outer area of a typical building, we find that the wall penetration loss obeys normal distribution with a mean of 24.31 dB. As a result, the geographical distribution of spatial spectrum holes is plotted indicating spatial spectrum holes are abundant in the outskirts of city. Spatial spectrum holes is very important since it can be utilized by short-range communication such as Wi-Fi or dense small cell deployment in 5G.

References

1. Islam, M.H., et al.: Spectrum survey in Singapore: occupancy measurements and analyses. In: Proc. 3rd Int. Conf. Crowncom, pp. 1–7 (2008)
2. Bao, V.N.Q., et al.: Vietnam spectrum occupancy measurements and analysis for cognitive radio applications. In: ATC, pp. 135–143 (2011)
3. FCC: Second report and order and memorandum opinion and order, pp. 8–260 (2008)
4. Chen, K., et al.: Spectrum Survey for TV Band in Beijing. In: 21st ICT, pp. 267–271 (2014)
5. COST 231 Final Report: Digital Mobile Radio Towards Future Generation Systems. COST Telecom Secertariat, Brussels (1999)
6. GB/T 26686–2011: General specification for digital terrestrial television receiver. Chinese Standards Press (2011)